J Mater Sci (2011) 46:734–738
DOI 10.1007/s10853-010-4805-9

Magnetic properties of La and (La, Zr) doped $BiFeO_3$ ceramics

Changyong Lan · Yuwen Jiang · Shaoguang Yang

Received: 23 March 2010 / Accepted: 27 July 2010 / Published online: 10 August 2010

Abstract $Bi_{0.9}La_{0.1}FeO_3$ (BLF) and $Bi_{0.9}La_{0.1}Fe_{0.98}Zr_{0.02}O_3$ (BLFZ) ceramics were synthesized by conventional solid state reaction method. X-ray diffraction studies and Rietveld refinements indicated that both of the samples possessed rhombohedrally distorted perovskite structure. The average grain size of BLFZ ($\sim$700 nm) was greatly reduced in comparison with BLF ($\sim$6 μm). The remanent magnetization of BLFZ was greatly enhanced compared with BLF. The enhancement of remanent magnetization was attributed to the collapse of the spiral spin structure. Both samples showed exchange bias. The possible reason for the appearance of exchange bias was attributed to the inhomogeneity in doping. The measurements of magnetization as a function of temperature indicated that BLF and BLFZ had almost the same magnetic transition temperature ($\sim$355 °C).

Introduction

Multiferroic materials are attracting much attention due to their potential applications and their fascinating fundamental physics [1–4]. However, there are very few single phase multiferroic materials, especially room temperature single phase multiferroic materials [1–4]. Among those single phase multiferroic materials, $BiFeO_3$ (BFO) is the most intensively studied material due to its high ferroelectric Curie temperature $T_C \sim 1103$ K and antiferromagnetic Néel temperature $T_N \sim 643$ K [5]. BFO possesses rhobomhedrally distorted perovskite structure with space group $R3c$ [6, 7]. The magnetic structure of BFO is antiferromagnetic with G-type spin ordering. Due to the magnetoelectric coupling, the two Fe^{3+} sublattices are canted, leading to a weak local net magnetization. However, the possible weak ferromagnetism is cancelled by the spiral spin structure with a period of 62 nm, which inhibits the observation of the linear magnetoelectric effect [8, 9]. A-site (Bi-site) substitution by lanthanide ions La^{3+} has been used to improve the multiferroic properties of BFO by many authors [10–14]. On the other hand, B-site (Fe-site) doping with high valence ions, such as Nb^{5+} and Ti^{4+}, can increase the resistivity of BFO, which allowed the ferroelectricity to be determined at room temperature [15, 16]. A-site and B-site co-doping is a good way to improve the multiferroic properties of BFO, both in films and ceramics [17–19]. Recently, it was reported that by co-doping with La^{3+} and Nb^{5+}, the magnetic properties of BFO can be greatly enhanced [18]. However, no investigations about La^{3+} and Zr^{4+} co-doped bulk materials were reported. In this work, we present that the remanent magnetization can be greatly enhanced by co-doping with La^{3+} and Zr^{4+} in BFO.

Experimental procedure

$Bi_{0.9}La_{0.1}FeO_3$ (BLF) and $Bi_{0.9}La_{0.1}Fe_{0.98}Zr_{0.02}O_3$ (BLFZ) ceramics were synthesized by solid state reaction method. Stoichiometric amounts of Bi_2O_3 (99.0%), La_2O_3 (99.99%), Fe_2O_3 (99.0%), and ZrO_2 (99.0%) were carefully weighed and thoroughly mixed in an agate mortar for 2 h. The mixture was calcined in an alumina crucible at 800 °C for 2 h in air followed by furnace cooling. It was then ground again and pressed into a disk. The disk was sintered at 850 °C for 2 h.

C. Lan · Y. Jiang · S. Yang (✉)
Nanjing National Laboratory of Microstructures and Department of Physics, Nanjing University, Nanjing 210093, China
e-mail: sgyang@nju.edu.cn

The phase purity and crystal structures were examined by X-ray diffractometer (XRD, X'Pert Philips) with Cu Kα radiation. Rietveld refinements were used to analyze XRD data using EXPGUI + GSAS program [20]. The surface morphologies of the ceramics were examined using scanning electron microscopy (SEM, Philips-XL30 operated at 20.0 kV). Magnetic properties were measured by vibrating sample magnetometer (VSM, ADE-EV7).

Results and discussion

Figure 1 shows the XRD patterns of BLF and BLFZ at room temperature. Small amount of impurities are detected in BLF, such as $Bi_2Fe_4O_9$ and $Bi_{25}FeO_{39}$ as labeled in Fig. 1. With the addition of 2 at.% Zr, the peaks belonging to impurities are substantially decreased. Only a weak peak belonging to $Bi_{25}FeO_{39}$ can still be observed. It can be found that the crystal structures of BLF and BLFZ are rhombohedrally distorted perovskite with space group *R*3*c*. No structure transition happens with the 2 at.% Zr doping at Fe-site to BLF, which is different from the monoclinic phase of $Bi_{0.9}La_{0.1}Fe_{0.98}Nb_{0.02}O_3$ ceramics reported in the Ref. [18]. In order to obtain the detailed crystal structure parameters of BLF and BLFZ ceramics, Rietveld refinements were used to analyze the XRD data of the two samples. The observed, calculated, and difference XRD patterns are given in Fig. 2. There is a good agreement between observed and calculated patterns. The detailed parameters obtained from Rietveld refinements are listed in Table 1. The lattice constants of BLFZ are larger than BLF, which is because the radius of Zr^{4+} is larger than Fe^{3+} (Zr^{4+}: 0.72 Å, high spin Fe^{3+}: 0.645 Å [21]). With the doping of 2 at.% Zr at Fe-site to BLF, the bond lengths of Fe–O are changed and the Fe–O–Fe angle is enlarged, which will affect the magnetic properties of BLF as discussed below in this paper.

The surface morphologies of BLF and BLFZ are shown in Fig. 3a and b, respectively. The average grain size of BLF is very large (~6 μm), but the average grain size of BLFZ decreases substantially and becomes more homogeneous (~700 nm). The same phenomenon has been observed in Mn^{4+} doped BFO ceramics and La^{3+}, Nb^{5+} co-doped BFO ceramics [18, 22]. As the doped ions possess a valence higher than +3, the addition of high valence ions at Fe^{3+} site requires charge compensation, which can be achieved by filling the oxygen vacancies. Thus, the reduced grain size can be interpreted by the suppression of oxygen vacancy concentration, which results in slower oxygen ion motion and consequently lower grain growth rate [22]. So the grain size of BLFZ is smaller than that of BLF.

The room temperature magnetic hysteresis loops of BLF and BLFZ are shown in Fig. 4a and b, respectively. Both samples show nonlinear magnetic hysteresis loops. BFO is antiferromagnetic with *G*-type spin configuration. The crystal structure of BFO permits the appearance of weak ferromagnetism arising from the canting of the antiferromagnetic sublattices [9]. However, the possible net magnetization is cancelled by the spiral spin structure. The appearance of remanent magnetization of BLF is attributed to the suppression of the spiral spin structure by 10 at.% La doping at Bi-site [10]. But the spiral spin structure of BFO is not completely destroyed by 10 at.% La doping [10, 14]. It can be seen that the remanent magnetization of BLFZ is greatly enhanced in comparison with BLF. The remanent

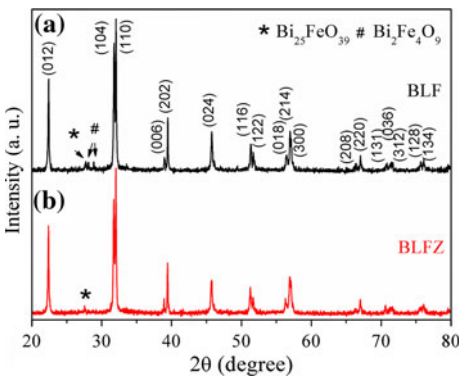

Fig. 1 XRD patterns of *a* BLF and *b* BLFZ at room temperature. The diffraction peaks corresponding to the impurities $Bi_{25}FeO_{39}$ and $Bi_2Fe_4O_9$ are marked by * and #, respectively. The XRD pattern of BLF and BLFZ are indexed according to *R*3*c* BFO (JCPDS No. 86-1518)

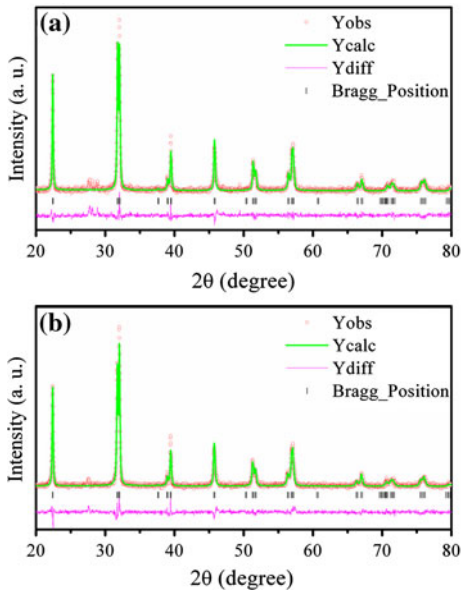

Fig. 2 The observed, calculated, and difference Rietveld refined XRD patterns of **a** BLF and **b** BLFZ

Table 1 Structural parameters of BLF and BLFZ

Samples	BLF	BLFZ
Lattice constants (Å)		
a	5.5823(1)	5.5854(1)
c	13.8479(5)	13.8685(6)
Cell volume (Å^3)	373.72(2)	374.69(2)
R-values of Rietveld refinements (%)		
R_{wp}	6.67	7.92
R_p	5.67	6.21
χ^2	1.232	1.158
Atomic position parameters		
Bi/La		
x	0	0
y	0	0
z	0	0
Fe/Zr		
x	0	0
y	0	0
z	0.2224	0.2213
O		
x	0.4444	0.4538
y	0.0050	0.0017
z	0.9570	0.9545
Interatomic distances (Å)		
Bi/La–O	2.5377	2.6072
	2.3572	2.3384
Fe/Zr–O	2.1205	2.1381
	1.9142	1.8832
Fe–O–Fe angle (°)	158.51	161.21

magnetization of BLFZ (0.013 emu/g) is similar to that of 30 at.% La doped BFO (0.02 emu/g) [10]. The enhanced remanent magnetization in 30 at.% is attributed to the destruction of spiral spin structure caused by structural transformation [10]. Thus, the spiral spin structure in BLFZ might be destroyed, but the reason for the destruction of the spiral spin structure is different. As known to us, there is no magnetic interaction between Zr^{4+} and Fe^{3+} since Zr^{4+} is nonmagnetic, but a small amount of Zr^{4+} doping at Fe-site of BLF perturbs the superexchange interaction Fe–O–Fe. And the Fe–O–Fe angle and Fe–O distances are changed by Zr^{4+} doping as shown in Table 1. As the superexchange interaction is sensitive to bond angles and bond distances, the spiral spin structure might be destroyed completely by co-doping of La^{3+} and Zr^{4+}, which leads to the release of latent magnetization and the enhancement of remanent magnetization in BLFZ. Although the remanent magnetization is enhanced, the high field values of the magnetization are similar for BLF and BLFZ. This indicates that the nature of canting antiferromagnetic sublattices does not

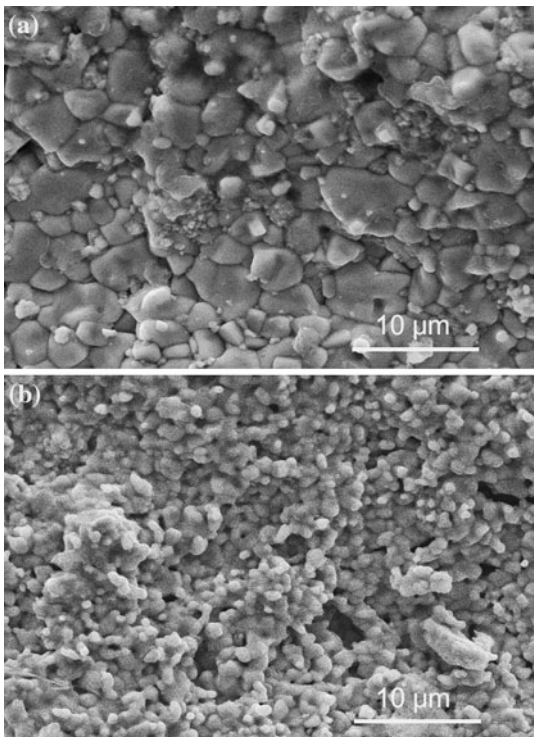

Fig. 3 SEM images of the surface of the samples **a** BLF and **b** BLFZ

be changed by doping. The magnetic hysteresis loop of BLFZ shows a very large coercive field (1686 Oe) in comparison with BLF (254 Oe). The reason for the increased coercive field of BLFZ may be attributed to the decreased grain size in the BLFZ sample, as reported in $Bi_{0.9}La_{0.1}Fe_{0.98}Nb_{0.02}O_3$ ceramics (~500 nm) [18]. The grain size of BLFZ might be close to the single magnetic domain size and as a result the coercivity is enhanced [18].

The insets of Fig. 4a and b show exchange bias in both samples. A similar phenomenon has been observed in La doped BFO ceramics before, but the reason is still not very clear [12]. One possible reason here might be the inhomogeneity in doping. The inhomogeneous mixing of the starting oxides may cause inhomogeneous doping of La and Zr in the samples, leading to the richer distribution of La and Zr at the grain boundaries as reported in Li and Ti doped NiO ceramics [23]. As a consequence, the inner side of a grain is antiferromagnetic while the boundary of the grain is weak ferromagnetic. Thus, the exchange bias appears.

The temperature dependence of magnetization of the samples was measured at a low magnetic field of 1000 Oe from room temperature to 500 °C to determine the magnetic ordering temperature as shown in Fig. 5. The magnetization of both samples shows a sharp decrease at around of ~355 °C, which is considered to be the magnetic transition temperature of the two samples. This transition temperature is close to the spin ordering

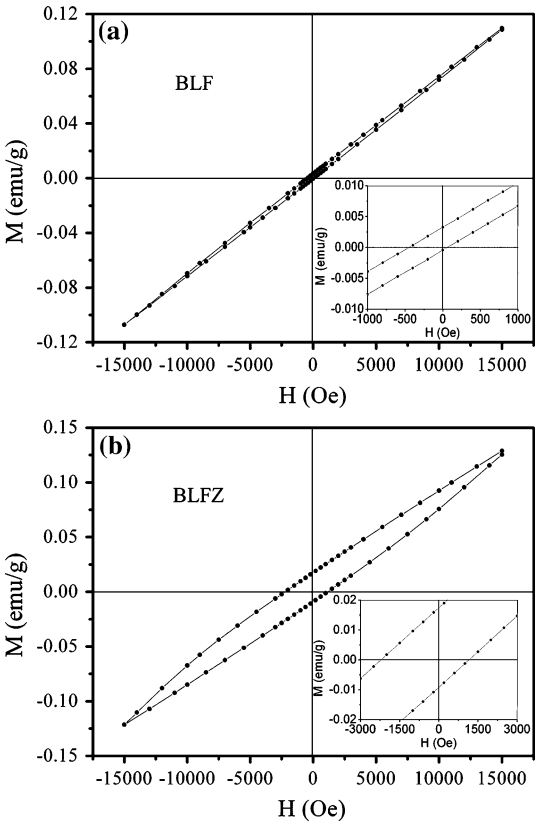

Fig. 4 Room temperature magnetic hysteresis loops of **a** BLF and **b** BLFZ. The *inset* of each graph shows the magnified part of the corresponding loop in the low field range

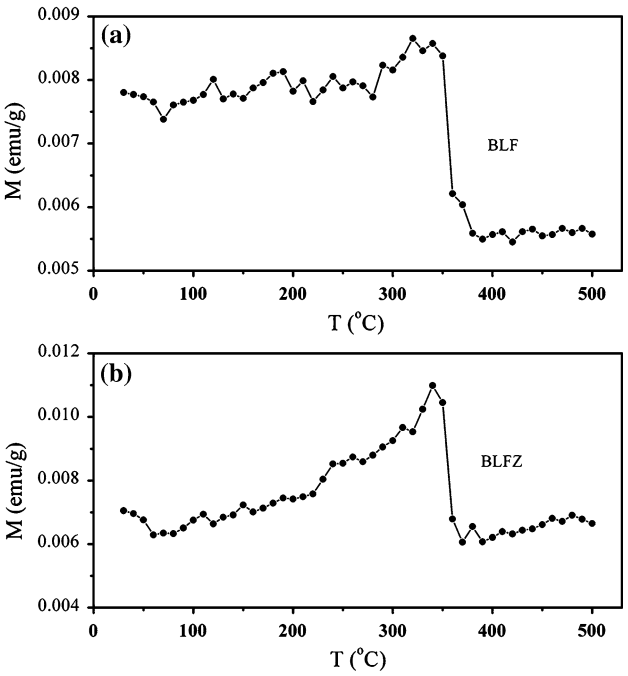

Fig. 5 Temperature dependence of magnetization of **a** BLF and **b** BLFZ. The applied magnetic field is 1000 Oe

temperature of BFO (~370 °C [5]). This result indicates that the addition of 2 at.% Zr at Fe-site to BLF does not affect the magnetic transition temperature too seriously, which is quite different from the case in La and Nb co-doped BFO ceramics [18]. The antiferromagnetic interaction seems enhanced in BLFZ since the increase of magnetization with temperature is faster than BLF. This result is attributed to the increase of Fe–O–Fe angle as listed in Table 1, since the increase of bond angle can enhance superexchange interaction between the two Fe ions [24]. Though the antiferromagnetic interaction is enhanced, the magnetic transition temperature of BLFZ remains almost the same with BLF. The transition temperature of $A^{3+}FeO_3$ type antiferromagnet depends on bond angle and bond length in a complex way [25]. The bond length and bond angle of BLFZ are all changed compared with BLF as shown in Table 1, thus the cooperation of those factors may lead to an unchanged spin ordering temperature.

Conclusions

The phase purity, structure, surface morphologies, and magnetic properties of BLF and BLFZ ceramics were investigated. Both of the samples showed rhombohedrally distorted perovskite structure with space group *R*3*c*. The grains of BLFZ were greatly reduced and became homogeneous in comparison with BLF. BLFZ showed much enhanced remanent magnetization, which was attributed to the collapse of the spiral spin structure. Exchange bias and large coercivity were observed in BLFZ. The Néel temperature of BLFZ remains the same with BLF (~355 °C).

Acknowledgements This work was supported by National Natural Science Foundation of China (10774068), Program for New Century Excellent Talents in University (07-0430), and National Basic Research Program of China (2009CB929501).

References

1. Fiebig M (2005) J Phys D Appl Phys 38:R123
2. Prellier W, Singh MP, Murugavel P (2005) J Phys Condens Matter 17:R803
3. Ramesh E, Spaldin NA (2007) Nat Mater 6:21
4. Wang KF, Liu JM, Ren ZF (2009) Adv Phys 58:321
5. Teague JR, Gerson R, James WJ (1970) Solid State Commun 8:1073
6. Michel C, Moreau JM, Achenbach GD, Gerson R, James WJ (1969) Solid State Commun 7:701
7. Kubel F, Schmid H (1990) Acta Crystallogr Sect B Struct Sci 46:698
8. Sosnowska I, Peterlin-Neumaier T, Steichele E (1982) J Phys C Solid State Phys 15:4835
9. Kadomtseva A, Zvezdin A, Popov Y, Pyatakov A, Vorob'ev G (2004) JETP Lett 79:571

10. Zhang ST, Pang LH, Zhang Y, Lu MH, Chen YF (2006) J Appl Phys 100:114108
11. Lin YH, Jiang QH, Wang Y, Nan CW (2007) Appl Phys Lett 90:172507
12. Das SR, Choudhary RNP, Bhattacharya P, Katiyar RS, Dutta P, Manivannan A, Seehra MS (2007) J Appl Phys 101:034104
13. Cheng ZX, Li AH, Wang XL, Dou SX, Ozawa K, Kimura H, Zhang SJ, Shrout TR (2008) J Appl Phys 103:07E507
14. Bras GL, Colson D, Forget A, Genand-Riondet N, Tourbot R, Bonville P (2009) Phys Rev B 80:134417
15. Jun YK, Moon WT, Chang CM, Kim HS, Ryn HS, Kim JW, Kim KH, Hong SH (2005) Solid State Commun 135:133–137
16. Kumar M, Yadav KL (2006) J Appl Phys 100:074111
17. Cheng ZX, Wang XL, Dou SX, Kimura H, Ozawa K (2008) Phys Rev B 77:092101
18. Zhai L, Shi YG, Tang SL, Lv LY, Dou YW (2009) J Phys D Appl Phys 42:165004
19. Yu BF, Li MY, Liu J, Guo DY, Pei L, Zhao XZ (2008) J Phys D Appl Phys 41:065003
20. Toby BH (2001) J Appl Crystallogr 34:210
21. Shannon RD (1976) Acta Crystallogr Sect A: Found Crystallogr 32:751
22. Kumar M, Yadav KL (2007) Appl Phys Lett 91:242901
23. Lin YH, Li M, Nan CW, Li JF, Wu JB, He JL (2006) Appl Phys Lett 89:032907
24. Lyubutin IS, Dmitrieva TV, Stepin AS (1999) J Exp Theor Phys 88:590
25. Goodenough JB (1967) Phys Rev 164:785